Catalysis Today xxx (2017) xxx-xxx

Contents lists available at ScienceDirect

Catalysis Today

journal homepage: www.elsevier.com

CO_2 reduction over Cu-ZnGaMO (M = Al, Zr) catalysts prepared by a sol-gel method: Unique performance for the RWGS reaction

Xianyun Liu[a, b], Pilar Ramírez de la Piscina[a], Jamil Toyir[b, c], Narcis Homs[a, b, *]

[a] Departament de Química Inorgànica i Orgànica, Secció Química Inorgànica and Institut de Nanociència i Nanotecnologia, Universitat de Barcelona, Martí i Franquès 1-11, 08028 Barcelona, Spain
[b] Catalonia Institute for Energy Research (IREC), Jardins de les Dones de Negre 1, 08930 Barcelona, Spain
[c] Université Sidi Mohamed Ben Abdellah Fès, FP-Taza, Laboratoire de Chimie de la Matière Condensée, Equipe de Procédés pour l'Energie et l'Environnement, BP 1223 Taza, Morocco

ARTICLE INFO

Keywords:
CO_2 reduction
RWGS
ZrO_2
Ga_2O_3
Cu-ZnO-based catalysts

ABSTRACT

Cu-ZnGaMO (M = Al, Zr) catalysts prepared by a surfactant-free sol-gel method were characterized and tested in the reverse water-gas shift (RWGS) reaction. Their catalytic behavior was analyzed under 0.1–3 MPa at 250–325 °C and using a reactant mixture of CO_2/H_2 = 1/3. The catalytic results are analyzed in the light of the characteristics of the catalysts. The Cu-ZnGaZrO catalysts were highly selective for the RWGS reaction; amajor role of surface copper and interface oxygen vacancies is proposed. CO_2 conversion and CO selectivity increased on increasing the reaction temperature. CO_2 conversion reaches 16.8% with 99.7% selectivity for CO under 0.1 MPa at 325 °C over the Cu-ZnGaZrO1 catalyst. It is suggested that CO and methanol production proceed via independent reaction pathways.

1. Introduction

Effective technologies for CO_2 capture and storage that are currently under development are predicted to be operative in a near future [1]. Therefore, abundant CO_2 could conveniently be available to be recycled through catalytic processes. In this context, the use of large-scale CO_2 conversion into strategic chemicals or fuels could be of particular interest [2,3]. One of the key steps in CO_2 conversion by reduction is its catalytic conversion to produce CO through the reverse water-gas shift (RWGS) reaction:

$$CO_2 + H_2 \leftrightarrow CO + H_2O \quad \Delta H = 41.2\ kJ/mol$$

The RWGS reaction is a promising process for CO_2 utilization, since it can be performed at relatively low pressures. From this process, the resulting mixture ($H_2/CO/CO_2$) could be further used as feedstock for well-known processes, like the Fischer-Tropsch process or methanol synthesis.

Cu- and Cu-ZnO-based catalysts have been widely used in the field of CO_2 hydrogenation reactions [2–7]. However, most work related to the use of Cu-ZnO-based catalysts in the CO_2/H_2 reaction focuses on methanol synthesis, and usually under methanol synthesis conditions, CO production through the RWGS reaction is detrimental to methanol selectivity. Besides the reaction conditions, the presence of different promoters and the preparation method are key factors in the catalytic behavior of Cu-ZnO-based catalysts in the CO_2/H_2 reaction. For Cu/ZnO catalysts prepared by coprecipitation, the CO_2 conversion has recently been correlated with the total amount of chemisorbed hydrogen which is the result of hydrogen spillover on ZnO_x and ZnO [8]. The theoretical concentration of Cu–ZnO contacts has been directly linked to CO_2 conversion [8]. However, the active sites for methanol and CO formation are believed to be different. In this context, catalysts constituted of Cu-ZnO_x core-shell structures are highly selective for CO-free methanol synthesis [8]. DFT analysis of the RWGS reaction on Cu (111) has shown that Cu tends towards the CO_2 dissociation mechanism for the conversion of CO_2 to CO rather than the COOH-mediated mechanism [9]. Meanwhile, the bonding capacity of atomic O with cations at the Cu–oxide interface could be the key for the increase in the selectivity for CO with respect to that of methanol when the CO_2/H_2 reaction takes place [10].

For different Cu-based catalysts used in methanol synthesis via CO_2 hydrogenation, a promoter effect of Ga_2O_3 in terms of catalyst stability has been reported [11–13]. Small particles of Ga_2O_3 have been re-

* Corresponding author at: Departament de Química Inorgànica i Orgànica, Secció Química Inorgànica and Institut de Nanociència i Nanotecnologia, Universitat de Barcelona, Martí i Franquès 1-11, 08028 Barcelona, Spain.
Email address: narcis.homs@qi.ub.edu, nhoms@irec.cat (N. Homs)

http://dx.doi.org/10.1016/j.cattod.2017.04.022
Received 15 January 2017; Received in revised form 28 March 2017; Accepted 10 April 2017
Available online xxx
0920-5861/

ported to favor the formation of an intermediate oxidation state of copper, probably Cu^+ [11,14].

Although the stabilization of Cu/SiO_2 catalysts used in the RWGS reaction at a high temperature (600 °C) by introduction of different promoters has been reported [15,16], the development of highly active Cu-based catalysts for low-temperature operation is very attractive. We recently reported the use of $CuOZnOGa_2O_3$ catalysts for H_2 production from methanol steam reforming (MSR) at low temperatures. We analyzed the effect of the addition of Al_2O_3 and ZrO_2 on the catalytic performance of $CuOZnOGa_2O_3$ catalysts for MSR; under MSR conditions at 250–275 °C, it has been suggested that CO formation on these systems would take place through the RWGS reaction [17]. In this paper, we report a study of multicomponent Cu-ZnO catalysts usedin the RWGS reaction. Cu-ZnO-based catalysts, containing Ga_2O_3 and Al_2O_3, and Ga_2O_3 and ZrO_2, and prepared using a surfactant-free sol-gel method [17], were studied in the CO_2/H_2 reaction in the 0.1–3 MPa and 250–325 °C ranges. The catalysts were characterized using X-ray diffraction (XRD), temperature programmed H_2-reduction (H_2-TPR), temperature programmed desorption of H_2 (H_2-TPD) and CO_2 (CO_2-TPD), X-ray photoelectron spectroscopy (XPS) and N_2O chemisorption.

2. Materials and methods

2.1. Catalyst preparation

Multicomponent catalysts containing Cu, ZnO, Ga_2O_3 and either ZrO_2 (Cu-ZnGaZrO) or Al_2O_3 (Cu-ZnGaAlO) were synthesized by a sol-gel method following a procedure described elsewhere [17,18]. Briefly, metal nitrate salts were separately dissolved in **an** aqueous solution of ethylene diamine tetraacetic acid (EDTA) and ethylene diamine (ED) mixtures; only the $ZrO(NO_3)_2$ precursor was dissolved in deionized water. Appropriate amounts of these solutions were then mixed in a beaker and kept in a thermostated bath at 60 °C to obtain a gel. Finally, this gel was heated under air, in an oven, at 200 °C for 4 h and subsequently at 500 °C for 4 h. Before use, the samples were reduced at 300 °C (for catalytic tests at 250–270 °C) or 325 °C (Cu-ZnGaZrO1 for the catalytic test at 275–325 °C) under a H_2/Ar (12% vol/vol) flow for 3 h. For comparative purposes, Cu-ZnO, ZnGaAlO and ZnGaZrO catalysts were also prepared using the same method.

2.2. Catalyst characterization

The chemical composition of the catalysts was determined by inductively-coupled plasma atomic emission spectroscopy (ICP-AES) using Perkin Elmer Optima 3200RL apparatus.

N_2 adsorption-desorption isotherms were recorded at −196 °C using a Micromeritics Tristar II 3020 equipment. Prior to the measurements, the samples were degassed at 250 °C for 5 h. The specific surface area (S_{BET}) was calculated by multi-point BET analysis of the nitrogen adsorption isotherms.

The XRD analysis was performed on a PANalytical X'Pert PRO MPD Alpha1 powder diffractometer equipped with $CuK\alpha_1$ radiation. The XRD profiles were collected between $2\theta = 4°$ and $2\theta = 100°$, with a step width of 0.017° and counting 50 s at each step. The mean crystallite sizes were calculated using the Debye-Scherrer equation.

H_2-TPR as well as both H_2-TPD and CO_2-TPD were carried out using a Micromeritics AutoChem HP2950 analyzer. For the H_2-TPR experiments, each calcined catalyst was pretreated at 90 °C under a flow of He. After cooling to room temperature, the samples were exposed to a H_2/Ar (12% vol/vol) flow, and the temperature was linearly increased at 10 °C/min up to 800 °C. For the H_2-TPD experiments, the samples were first treated under a He flow at 90 °C, then reduced at 300 °C for 2 h in a H_2/Ar (12% vol/vol) mixture. Then the catalysts were cooled to 50 °C and maintained for 0.5 h under the same H_2/Ar flow, and then flushed with Ar for 1 h. Finally, the temperature was linearly increased up to 500 °C at 5 °C/min. The outlet gases were monitored by massspectrometry (MS). Prior to the CO_2-TPD, the catalysts were first reduced under a H_2/Ar flow (12% vol/vol, 50 mL/min) for 2 h at 300 °C, and then cooled to 35 °C. The adsorption of CO_2 was carried out at 35 °C with a feed of CO_2/He (10% vol/vol) for 1 h. Then, the samples were flushed with He for 2 h and the temperature was increased under a He flow up to 500 °C at 5 °C/min.

The N_2O chemisorption experiments were carried out in a Micromeritics AutoChem II chemisorption analyzer. The catalysts were first reduced in a H_2/Ar (12% vol/vol) mixture at 275 °C, and then they were purged with He and cooled to 50 °C. The samples were flushed with a N_2O/He (6% vol/vol) mixture at 50 °C for 0.5 h, and then they were cooled under a He flow to room temperature to determine the H_2 consumption.

The XPS was performed in a Perkin Elmer PHI-5500 Multitechnique System (Physical Electronics) with an Al X-ray source ($h\nu$ = 1486.6 eV and 350 W). All the measurements were carried out in an ultra high vacuum chamber with a pressure in the $5{\cdot}10^{-9}$–$2{\cdot}10^{-8}$ torr range during data acquisition. The binding energy values were referred to that of C1s at 284.8 eV.

2.3. Catalytic tests

The RWGS reaction tests were performed in a Microactivity-Reference unit (PID Eng&Tech) with a tubular fixed-bed reactor, using 150 mg of sample diluted with inactive SiC up to a total volume of 1 mL. The reaction temperature was measured by a thermocouple in direct contact with the catalyst bed. Before reaction, the catalysts were sieved at 0.2–0.4 mm, they were in-situ reduced in a H_2/Ar (12% vol/vol) stream at 300 °C for 2 h under atmospheric pressure and then at 3 MPa for 1 h. Afterwards, the pressure was kept at 3 MPa and the temperature was decreased to 240 °C; then the samples were exposed to a reactant mixture of $CO_2/H_2/N_2$ (1/3/1 molar ratio) under a gas hourly space velocity (GHSV) of 3000 h^{-1} and the reaction temperature was increased to 250 °C. After a period of ca. 15 h, the reaction temperature was consecutively increased to 260 °C and 270 °C and maintained for ca. 5 h at each temperature. The influence of contact time over the Cu-ZnGaZrO1 catalyst was analyzed in separate experiments carried out at 270 °C and 3 MPa by varying the GHSV in the range 48,000–10,000 h^{-1}; the influence of pressure over the Cu-ZnGaZrO1 catalyst was studied in the range 0.1-3 MPa at 270 °C and GHSV of 3000 h^{-1}. The catalytic behavior of Cu-ZnGaZrO1 was also studied at 0.1 MPa in the 275–325 °C range under GHSV = 3000 h^{-1}. The Cu-ZnGaZrO1 sample was pre-reduced at 325 °C for 3 h at atmospheric pressure before being exposed to the $CO_2/H_2/N_2$ (1/3/1 molar ratio) reactant mixture. In all cases, after each change the system was stabilized for 1 h before the first analysis was carried out. The products were analyzed on-line using a Varian 450-GC–MS equipped with a methanizer and TCD, FID and mass detectors. CO and CO_2 were separated and converted into methane using an appropriate methanizer, and then the CH_4 formed analyzed by FID.

The CO_2 conversion (XCO_2) and selectivity (S_i) for each product was defined as follows:

$$XCO_2\,(\%) = \left(1 - \frac{(C_{CO_2})_{outlet}}{(C_{CO_2})_{outlet} + n * \sum (Ci)_{outlet}}\right) \times 100$$

$$S_i\,(\%) = \frac{(Ci)_{outlet}}{\sum (Ci)_{outlet}} \times 100$$

Where $(C_i)_{outlet}$ is the molar concentration of the product "i" in the effluent, and n is the number of carbon atoms in the product.

3. Results and discussion

As stated in the experimental section, in this work the performance of Cu-ZnO-based catalysts containing Ga_2O_3 and either ZrO_2 (Cu-ZnGaZrO), or Al_2O_3 (Cu-ZnGaAlO) was studied in the CO_2/H_2 reaction over the 0.1–3 MPa and 250–325 °C ranges. Moreover, two samples of ZnGaAlO and ZnGaZrO, without Cu, and the bare catalyst Cu-ZnO were studied for comparison. Table 1 shows the chemical composition and S_{BET} values of the catalysts. The S_{BET} of the Cu-ZnGaMO (M = Al, Zr) catalysts is higher than that of bare Cu-ZnO. Moreover, for a similar Ga_2O_3 content, the corresponding S_{BET} of the Cu-ZnGaZrO is higher than that of the Cu-ZnGaAlO catalyst. Fig. 1 shows the corresponding H_2-TPR profiles up to 500 °C; only the samples CuO containing show H_2 consumption peaks in this range of temperature. The amount of H_2 consumed appears in Table 1. From the results of the H_2 consumed, the total reduction of Cu^{2+} species can be proposed. However, a minor contribution related to the reduction of other species in the catalysts could not be ruled out. The H_2 consumption peaks of the Cu-ZnGaZrO and Cu-ZnGaAlO catalysts were broader than that of Cu-ZnO. The presence of several relative maxima in the H_2-TPR profiles of the Cu-ZnGaZrO and Cu-ZnGaAlO catalysts could be related with the existence of different interactions between the CuO particles and the various oxide components of the catalysts. The peaks at about 190–195 °C could be related to the reduction of small CuO particles with a moderate strength interaction with the support; the presence of oxygen vacancies at the CuO–oxide interface could facilitate the reduction of CuO species. From the H_2-TPR profiles in Fig. 1, mainly the presence of small CuO particles in Cu-ZnGaZrO catalysts can be inferred, the shoulder at 190 °C in the pattern of Cu-ZnGaAlO2 could also be indicative of the presence of a smaller amount of small CuO particles in this catalyst. Meanwhile, the Cu-ZnGaAlO1 catalyst shows the maximum of the H_2 consumption peak at the highest temperature, suggesting the presence of larger CuO particles or a stronger interaction between Cu^{2+} and the corresponding oxides in this catalyst.

The XRD patterns of the reduced catalysts containing Cu appear in Fig. 2a. In all cases, characteristic peaks of cubic Cu (JCPDS 00-004-0836) are observed. As in the case of the calcined samples (XRD patterns not shown), except for Cu-ZnGaAlO2, the presence of hexagonal ZnO (JCPDS 03-065-3411) can be deduced from the XRD patterns. The XRD pattern of Cu-ZnGaAlO2 shows peaks which could be assigned to the presence of $ZnAl_2O_4$ (JCPDS 00-005-0669) or $CuAl_2O_4$ (JCPDS 01-076-2295) with a spinel structure (MAl_2O_4); both $ZnAl_2O_4$ and $CuAl_2O_4$ show similar XRD patterns. However, the presence of $CuAl_2O_4$ in Cu-ZnGaAlO2 can be ruled out in accordance with the H_2-TPR results [19]. Peaks related to the presence of crystalline Ga_2O_3 were not detected in any case. The shoulder of a low intensity at about 2θ = 30.2° in the patterns of the Cu-ZnGaZrO catalysts could be related to the most intense diffraction peak of tetragonal (JCPDS 01-080-0784) or cubic (JCPDS 00-027-0997) ZrO_2. Meanwhile, from the XRD patterns of the Cu-ZnGaAlO catalysts, no presence of crystalline Al_2O_3 can be deduced.

Table 2 presents the crystallite sizes of the Cu and ZnO phases calculated from the XRD patterns using the Scherrer equation and the (111) Cu and (110) ZnO diffraction peaks at 2θ = 43.3° and 2θ = 56.6°, respectively. For Cu-ZnGaAlO2, it was not possible to estimate the Cu crystallite size due to the proximity of the (111) Cu peak and (400) peak of $ZnAlO_4$. Before reduction, the crystallite sizes of CuO and MAl_2O_4 in Cu-ZnGaAlO2 calculated using the Scherrer equation and the (111) CuO and (511) MAl_2O_4 peaks were 21.7 nm and 13.1 nm, respectively.

After reduction of the catalysts, N_2O chemisorption was performed. Although N_2O chemisorption has been extensively used for the quantification of the Cu^{00} on the surface of catalysts, it has recently been demonstrated that this method quantifies not only the Cu^{00} surface area, but also the oxygen defects which are present at the Cu–ZnOx interface of the $Cu/ZnO/Al_2O_3$ and Cu/ZnO/MgO catalysts [20]. Table 2 shows the values of H_2 consumption after N_2O chemisorption. The bare Cu-ZnO catalyst shows the lowest value of H_2 consumption, indicating that after N_2O chemisorption, this is the catalyst with the fewest reducible species (Cu_2O from surface Cu and reducible oxide species at the Cu–support interface). For Cu-ZnGaAlO and Cu-ZnGaZrO, an increase in the Ga content up to 6%–7% produces an increase in the H_2 consumption. For a similar content of Ga, the corresponding Cu-ZnGaZrO shows a higher H_2 consumption than Cu-ZnGaAlO. As stated above, Cu-ZnGaZrO materials show very well-defined peaks at lower reduction temperatures than their Cu-ZnGaAlO counterparts (Fig. 1). These findings indicate that Cu particles of a smaller size could be present in Cu-ZnGaZrO in which ZrO_2 and Ga_2O_3 could favor the Cu dispersion and enable CuO species to be more easily reduced [21]. Moreover, the presence of ZrO_2 and/or Ga_2O_3 could increase the number of oxygen defects at the Cu–support interface and therefore the H_2 consumption after N_2O chemisorption.

Fig. 3 shows the H_2-TPD profiles of the reduced catalysts. Studies of the H_2 interaction with Cu have shown that Cu can dissociatively adsorb H_2 on its surface and subsurface; the desorption of surface H has been reported to take place at about 27 °C [20,22] while subsurface H desorbs at about 287 °C [22]. For Cu-ZnO-based catalysts, peaks at about 100–120 °C have been related with atomic H on highly defective ZnO at the Cu/ZnO interface [22], and peaks at 350–500 °C with desorption of H_2 from bulk Cu particles or the ZnO surface [23,24]. Moreover, the dissociative chemisorption of H_2 on Ga_2O_3 has been observed at temperatures above 227 °C; heterolytic adsorption of H_2 at Ga-O-Ga sites produces OH and Ga-H, which can recombine and desorb as molecular H_2 at temperatures of 400 °C or higher [25].

Cu-ZnGaZrO and Cu-ZnGaAlO show two zones of H_2 desorption with maxima at 104–125 °C and 352–382 °C (Fig. 3). Meanwhile, ZnGaZrO and ZnGaAlO do not show peaks in the low-temperature zone. Peaks with a maximum at 104–125 °C could be related to the

Table 1
Chemical composition and S_{BET} of reduced catalysts. Hydrogen consumption during H_2-TPR experiments of calcined catalysts.

Catalyst	wt%			S_{BET} (m^2/g)	H_2/Cu (mol/mol)
	Cu	Al_2O_3 or ZrO_2	Ga_2O_3		
Cu-ZnO	34.3	–	–	12.7	0.98[a]
Cu-ZnGaAlO1	30.4	19.3	3.0	21.0	1.15
Cu-ZnGaAlO2	23.1	38.3	6.0	40.9	1.18
Cu-ZnGaZrO1	33.2	25.0	3.0	45.5	1.08[a]
Cu-ZnGaZrO2	23.6	36.2	7.2	52.2	1.09[a]
ZnGaAlO	–	36.1[b]	2.3[b]	–	–
ZnGaZrO	–	37.6[b]	2.4[b]	–	–

[a] From Ref. [17].
[b] Determined for calcined samples.

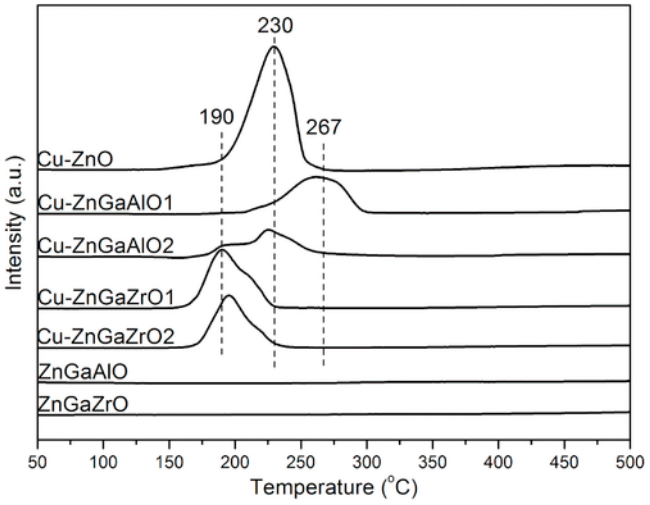

Fig. 1. H_2-TPR profiles of calcined catalysts. Data for Cu-ZnO, Cu-ZnGaZrO1 and Cu-ZnGaZrO2 from Ref. [17].

presence of Cu, probably with atomic H on highly deficient oxide (ZnO, Ga_2O_3 or ZrO_2) at the Cu–support interface. Peaks with a maximum in the zone 352–382 °C could be ascribed to the adsorption of H_2 on the support. The intensity of the peaks corresponding to Cu-ZnO was very much lower than those of Cu-ZnGaZrO and Cu-ZnGaAlO (Fig. 3), indicating a higher capacity of the multicomponent catalysts for H_2 adsorption. Moreover, for Cu-ZnGaZrO and Cu-ZnGaAlO, an increase in the Ga content produced an increase in the corresponding intensity of the peaks; both the capacity of Ga_2O_3 for H_2 adsorption [25] and the change of the Cu–support interface with the variation of Ga_2O_3 content could account for.

Fig. 4 shows the CO_2-TPD profiles corresponding to the different catalysts. Cu-ZnGaZrO and Cu-ZnGaAlO showed a higher number of surface basic sites of weak and medium strength than Cu-ZnO.

The surface atomic composition determined by XPS of the reduced Cu-containing catalysts is shown in Table 3. The Cu-ZnGaAlO catalysts showed significantly lower surface Cu concentrations than the other catalysts, while Cu-ZnO and Cu-ZnGaZrO showed similar surface Cu concentrations. The main component on the surface of the reduced Cu-ZnGaAlO catalysts is related with species containing Al.

Table 4 shows the behavior of the catalysts in the hydrogenation of CO_2 at 3 MPa and 250–270 °C. Results corresponding to ZnGaAlO and ZnGaZrO are also included in Table 4; however, they will not be further discussed due to the low values of CO_2 conversion achieved with them. For Cu-containing catalysts, in all cases, the CO_2 conversion increased with the increase in temperature. CO, CH_3OH and minor amounts of CH_4 were obtained as products. CO was always the major product and its yield depended on the catalyst. As expected, for a given catalyst, the CO selectivity increased and the CH_3OH selectivity decreased with the increase in temperature (Table 4). The Cu-ZnGaZrO catalysts were more active than their Cu-ZnGaAlO counterparts. As discussed above, the XPS and N_2O chemisorption results indicate that the Cu-ZnGaZrO catalysts presented much higher % mol Cu on the surface (Table 3) and a larger amount of reducible oxide species at the Cu–support interface than the Cu-ZnGaAlO catalysts (Tables 2 and 3). Cu-ZnGaZrO also showed a higher CO yield than Cu-ZnO in the overall temperature range analyzed. Although Cu-ZnGaZrO and Cu-ZnO showed similar %Cu on the surface (Table 3), the Cu-ZnGaZrO catalysts have much higher BET surface area values and much larger amounts of reducible oxide species at the Cu–support interface than Cu-ZnO. We propose that synergy involving the surface Cu and the

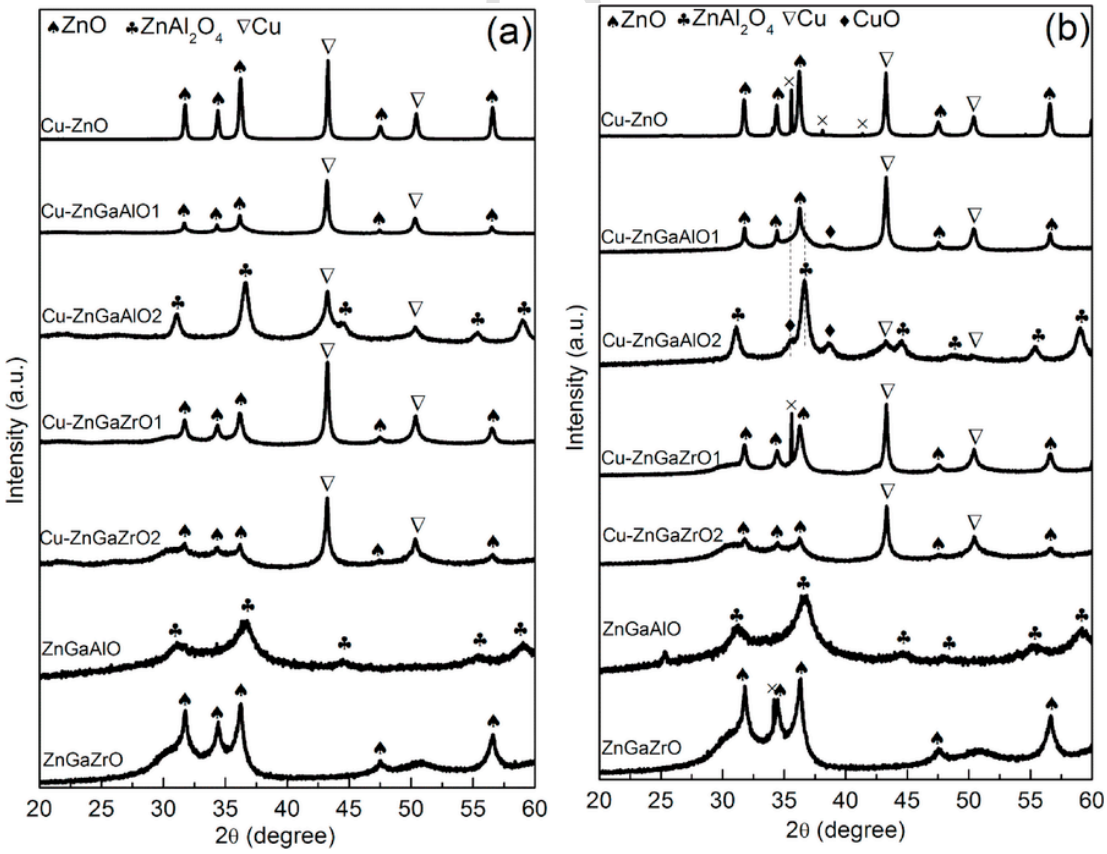

Fig. 2. XRD patterns: (a) H_2-reduced catalysts, (b) post-reaction catalysts. (♠), ZnO; (♣), $ZnAl_2O_4$ and/or $CuAl_2O_4$; (▽), Cu; (♦), CuO; × signals correspond to impurities of SiC.

Table 2
Crystallite size of Cu and ZnO calculated from XRD of reduced and post-reaction catalysts. H_2 consumption after N_2O chemisorption.

Catalyst	Reduced			Post-reaction	
	XRD		H_2 consumption after N_2O (μmol/g_{cat})	XRD	
	d_{Cu} (nm)	d_{ZnO} (nm)		d_{Cu} (nm)	d_{ZnO} (nm)
Cu-ZnO	46.8	35.3	197	39.4	34.2
Cu-ZnGaAlO1	32.2	38.5	258	27.9	33.4
Cu-ZnGaAlO2	n.d.	(14.7)[a]	292	n.d.	(14.6)[a]
Cu-ZnGaZrO1	30.0	24.6	415	31.5	23.8
Cu-ZnGaZrO2	25.9	19.2	421	29.5	23.0
ZnGaAlO	–	(4.0)[a,b]	–	–	(4.2)[a]
ZnGaZrO	–	16.1[b]	–	–	13.8

n.d.: not determined.
[a] $ZnAl_2O_4$ phase.
[b] Determined for calcined samples.

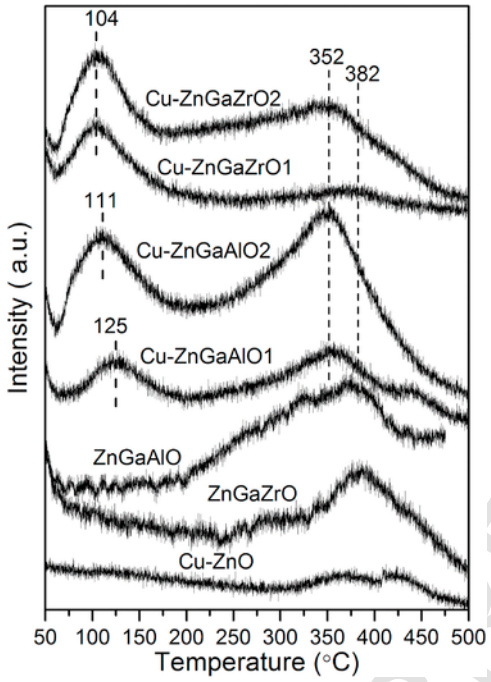

Fig. 3. H_2-TPD profiles of reduced catalysts as a function of desorption temperature.

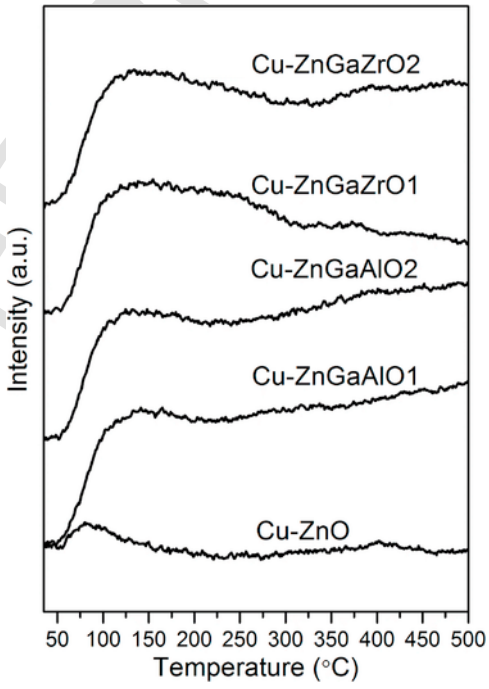

Fig. 4. CO_2-TPD profiles of reduced catalysts as a function of desorption temperature.

oxygen vacancies at the Cu–support interface is responsible for the better performance in the RWGS reaction of Cu-ZnGaZrO with respect to the Cu-ZnO or Cu-ZnGaAlO samples. For binary Cu/ZnO catalysts, an important role of optimized Cu/ZnO interfaces in the activation and dissociation of CO_2 as the rate determining step of the RWGS reaction has recently been proposed [26].

The post-reaction catalysts were analyzed by XRD. As shown in Fig. 2b, for all Cu-containing samples, metallic Cu and ZnO were observed. Moreover, for the Cu-ZnGaAlO catalysts, the presence of CuO and $ZnAl_2O_4$ phases cannot be ruled out. The calculated crystallite sizes for the different phases are presented in Table 2.

There were no large differences observed in the particle size of the different phases for the post-reaction catalysts compared to the corresponding reduced fresh catalysts.

The Cu-ZnGaZrO1 catalyst, which showed the highest CO production, was chosen for further analysis of different aspects of the reaction. In order to study on the relationship, if any, between CO and methanol formation, we analyzed the influence of the contact time during the RWGS reaction on the catalytic performance of Cu-ZnGaZrO1 at 270 °C under a total pressure of 3 MPa. This new experiment was carried out

Table 3
Surface atomic concentration of reduced catalysts determined by XPS analysis.

Catalyst	mol/mol (%)			
	Cu	Zn	Ga	Al or Zr
Cu-ZnO	11.6	88.4	–	–
Cu-ZnGaAlO1	4.5	24.1	2.8	68.6
Cu-ZnGaAlO2	6.6	14.6	3.3	75.5
Cu-ZnGaZrO1	11.6	45.5	4.9	37.9
Cu-ZnGaZrO2	12.7	27.9	7.5	51.9

by varying the GHSV from 10,000 h^{-1} up to 48,000 h^{-1}. Fig. 5 shows the CO_2 conversion and the CO and methanol selectivity values as a function of the contact time. CO_2 conversion increased from 5.5% to 12.6% with the increase in contact time, while only slight changes on CO and methanol selectivities were observed. These results suggest that CO and methanol are primary products formed through independent reaction pathways. However, we cannot rule out that a small fraction of the CO formed could come from the decomposition of methanol (Fig. 5).

Table 4
Catalytic behavior in RWGS reaction. CO_2 conversion (X_{CO_2}), CO yield, and CH_3OH (S_{CH_3OH}) and CH_4 (S_{CH_4}) selectivity values. Reaction conditions: T = 250–270 °C, P = 3 MPa, $CO_2/H_2/N_2$ = 1/3/1, GHSV = 3000 h^{-1}.

Catalysts	T(°C)	X_{CO_2} (%)	CO yield mmol/Kg h	S_{CH_3OH} (%)	S_{CH_4} (%)
Cu-ZnO	250	2.4	3354	14.0	< 0.01
	260	3.9	5817	8.6	0.01
	270	5.3	8098	6.8	0.01
Cu-ZnGaAlO1	250	1.5	1634	33.9	1.1
	260	1.9	2141	28.3	1.3
	270	2.6	3319	21.9	1.4
Cu-ZnGaAlO2	250	2.6	3879	9.4	0.03
	260	4.6	7061	6.4	0.03
	270	7.5	11,788	4.2	0.04
Cu-ZnGaZrO1	250	6.5	9226	12.7	0.2
	260	7.9	11,635	10.1	0.1
	270	11.2	17,047	6.9	0.1
Cu-ZnGaZrO2	250	5.8	8050	14.5	0.01
	260	7.0	10,133	11.8	0.02
	270	9.5	14,321	8.2	0.02
ZnGaAlO	250	0.1	137	18.9	1.9
	260	0.2	207	19.1	1.7
	270	0.2	317	18.7	1.4
ZnGaZrO	250	0.1	82	28.9	4.0
	260	0.1	118	28.0	3.8
	270	0.2	179	27.8	3.5

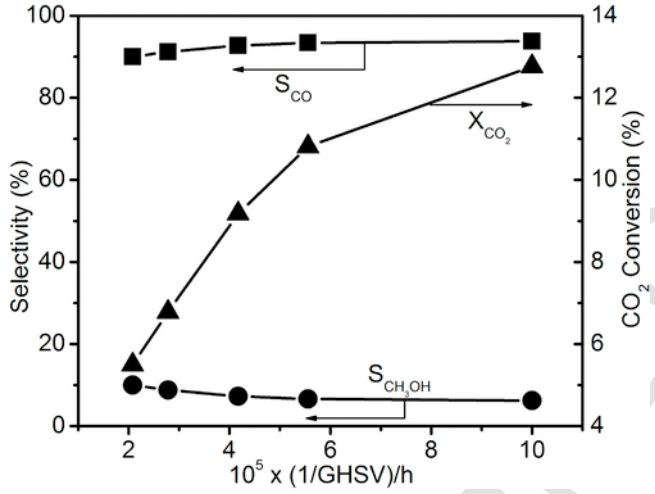

Fig. 5. Effect of GHSV variation on CO_2 conversion (X_{CO_2}), and CO (S_{CO}) and CH_3OH (S_{CH_3OH}) selectivity values over Cu-ZnGaZrO1. Reaction conditions: T = 270 °C, P = 3 MPa, GHSV = 10,000–48,000 h^{-1}.

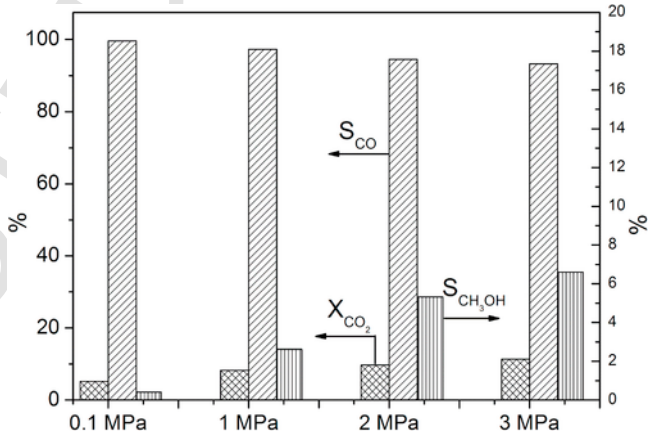

Fig. 6. CO_2 conversion ( ), and CO ( ) and CH_3OH ( ) selectivity values as a function of reaction pressure (0.1 MPa–3 MPa) over Cu-ZnGaZrO1; T = 270 °C.

We also studied the effect of the total pressure on the catalytic behavior of Cu-ZnGaZrO1. Fig. 6 shows the results as a function of pressure from 0.1 MPa to 3 MPa; the new experiment was performed at 270 °C under a GHSV of 3000 h^{-1}. As can be seen in Fig. 6, CO_2 conversion and CH_3OH selectivity increased with increasing reaction pressure. Although the increase in pressure from 0.1 MPa to 3 MPa increased the yield of both methanol and CO, the increase in the yield of methanol was very much greater than that of CO, in agreement with the expected effect of pressure in the RWGS and methanol synthesis reactions. Under these conditions, selectivity for CH_4 was always below 0.2%.

Finally, the RWGS reaction was also studied over Cu-ZnGaZrO1 in the 275–325 °C range at 0.1 MPa under a GHSV of 3000 h^{-1}. As can be observed in Table 5, CO production increased with the increase in temperature. Moreover, at temperatures higher than 275 °C, negligible selectivity for methanol was obtained while CO selectivity approached 100%. At 325 °C, the Cu-ZnGaZrO1 catalyst achieved a CO_2 conversion of 16.8%, compared to the expected CO_2 equilibrium conversion of 26.5%. For CO production over Cu-ZnGaZrO1, an apparent activation energy of 70.9 ± 3.7 kJ/mol was determined from the corresponding Arrhenius plot in the 275–325 °C range; this value is similar to that previously reported for $CuZrO_2CeO_2$ catalysts with similar Cu content [27]. For Cu/ZnO:Al and Cu/ZnO:Ga catalysts with a lower Cu content (approx. 10 wt%) and prepared by impregnation, apparent activation energy values of 112 kJ/mol in the 190–250 °C range have recently been reported [28].

Table 5
Catalytic behavior in RWGS reaction at 0.1 MPa of Cu-ZnGaZrO1. Reaction conditions: GHSV = 3000 h^{-1}, $CO_2/H_2/N_2$ = 1/3/1.

T(°C)	X_{CO_2} (%)	CO yield mmol/Kg h	S_{CO} (%)	S_{CH_3OH} (%)	S_{CH_4} (%)
325	16.8	27,415	99.7	< 0.01	0.3
300	9.6	15,612	99.8	< 0.02	0.2
275	4.6	7472	99.7	0.2	0.1

4. Conclusions

Multicomponent Cu-ZnO-based catalysts, containing Ga_2O_3 and either Al_2O_3 (Cu-ZnGaAlO) or ZrO_2 (Cu-ZnGaZrO), prepared using a surfactant-free sol-gel method are highly efficient in the RWGS reaction at 250–270 °C and 3 MPa using a CO_2/H_2 = 1/3 reactant mixture. Besides CO as the major product, CH_3OH and minor amounts of CH_4 were found. An increase in temperature from 250 °C to 270 °C produced an increase in both the conversion of CO_2 and selectivity for the RWGS reaction. Over the Cu-ZnGaZrO1 catalyst, CO and methanol are proposed to be the primary products formed through independent reaction routes.

The Cu-ZnGaZrO catalysts are more active in the RWGS reaction than the Cu-ZnGaAlO catalysts. This is related to a higher % mol Cu on the surface and a higher amount of surface reducible oxide species on Cu-ZnGaZrO than Cu-ZnGaAlO; the presence of more interface oxygen vacancies on Cu-ZnGaZrO is suggested.

The RWGS reaction carried out at 0.1 MPa and 325 °C over the Cu-ZnGaZrO1 catalyst achieves 16.8% CO_2 conversion and approaches 100% CO selectivity; an apparent activation energy of 70.9 ± 3.7 kJ/mol was determined at 275–325 °C.

Acknowledgements

The authors are grateful to the projects Consolider Ingenio 2010 MulticatCSD2009-00050 and MAT2014-52416-P for financial support. X.L. acknowledges a PhD grant from the China Scholarship Council and the University of Barcelona (IN2UB).

References

[1] F.C. Krebs, Energy Environ. Sci. 5 (2012) 7238–7239.
[2] M. Aresta, Carbon Dioxide as Chemical Feedstock, John Wiley & Sons, 2010.
[3] N. Homs, J. Toyir, P. Ramírez de la Piscina, Chapter 1–catalytic processes for activation of CO_2, in: S.L. Suib (Ed.), New and Future Developments in Catalysis: Activation of Carbon Dioxide, Elsevier, 2013.
[4] L.C. Grabow, M. Mavrikakis, ACS Catal. 1 (2011) 365–384.
[5] F. Arena, G. Mezzatesta, G. Zafarana, G. Trunfio, F. Frusteri, L. Spadaro, J. Catal. 300 (2013) 141–151.
[6] J. Graciani, K. Mudiyanselage, F. Xu, A.E. Baber, J. Evans, S.D. Senanayake, D.J. Stacchiola, P. Liu, J. Hrbek, J.F. Sanz, Science 345 (2014) 546–550.
[7] M.D. Porosoff, B. Yan, J.G. Chen, Energy Environ. Sci. 9 (2016) 62–73.
[8] C. Tisseraud, C. Comminges, T. Belin, H. Ahouari, A. Soualah, Y. Pouilloux, A. Le Valant, J. Catal. 330 (2015) 533–544.
[9] L. Dietz, S. Piccinin, M. Maestri, J. Phys. Chem. C 119 (2015) 4959–4966.
[10] Q.-L. Tang, Q.-J. Hong, Z.-P. Liu, J. Catal. 263 (2009) 114–122.
[11] J. Toyir, P. Ramírez de la Piscina, J.L.G. Fierro, N. Homs, Appl. Catal. B: Environ. 34 (2001) 255–266.
[12] W. Cai, P. Ramírez de la Piscina, J. Toyir, N. Homs, Catal. Today 242 (2015) 193–199.
[13] P.B. Sanguineti, M.A. Baltanás, A.L. Bonivardi, Appl. Catal. A: Gen. 504 (2015) 476–481.
[14] J. Toyir, P. Ramírez de la Piscina, J.L.G. Fierro, N. Homs, Appl. Catal. B: Environ. 29 (2001) 207–215.
[15] C.-S. Chen, W.-H. Cheng, S.-S. Lin, Appl. Catal. A: Gen. 257 (2004) 97–106.
[16] C.-S. Chen, W.-H. Cheng, S.-S. Lin, Appl. Catal. A: Gen. 238 (2003) 55–67.
[17] X. Liu, J. Toyir, P. Ramírez de la Piscina, N. Homs, Int. J. Hydrogen Energy (2017) http://dx.doi.org/10.1016/j.ijhydene.2016.12.133. in press.
[18] T. Mathew, K. Sivaranjani, E.S. Gnanakumar, Y. Yamada, T. Kobayashi, C.S. Gopinath, J. Mater. Chem. 22 (2012) 13484–13493.
[19] M.-F. Luo, P. Fang, M. He, Y.-L. Xie, J. Mol. Catal. A: Chem. 239 (2005) 243–248.
[20] M.B. Fichtl, J. Schumann, I. Kasatkin, N. Jacobsen, M. Behrens, R. Schlögl, M. Muhler, O. Hinrichsen, Angew. Chem. Int. Ed. 53 (2014) 7043–7047.
[21] J. Xiao, D. Mao, X. Guo, J. Yu, Appl. Surf. Sci. 338 (2015) 146–153.
[22] K. Waugh, Solid State Ion. 168 (2004) 327–342.
[23] F. Arena, G. Italiano, K. Barbera, S. Bordiga, G. Bonura, L. Spadaro, F. Frusteri, Appl. Catal. A: Gen. 350 (2008) 16–23.
[24] P. Gao, F. Li, N. Zhao, F. Xiao, W. Wei, L. Zhong, Y. Sun, Appl. Catal. A: Gen. 468 (2013) 442–452.
[25] S.E. Collins, M.A. Baltanás, A.L. Bonivardi, Langmuir 21 (2005) 962–970.
[26] C. Álvarez Galván, J. Schumann, M. Behrens, J.L.G. Fierro, R. Schlögl, E. Frei, Appl. Catal. B: Environ. 195 (2016) 104–111.
[27] A. Mastalir, B. Frank, A. Szizybalski, H. Sorijanto, A. Deshpande, M. Niederberger, R. Schomäcker, R. Schlögl, T. Ressler, J. Catal. 230 (2005) 464–475.
[28] J. Schumann, M. Eichelbaum, T. Lunkenbein, N. Thomas, C. Álvarez Galván, R. Schlögl, M. Behrens, ACS. Catal. 5 (2015) 3260–3270.